Isotope Exchange in Ionised CO_2/CO Mixtures: The Role of Asymmetrical $C_2O_3^+$ Ions

Giulia de Petris,*[a] Antonella Cartoni,[a] Marzio Rosi,[b] Anna Troiani,[a] Giancarlo Angelini,[c] and Ornella Ursini[c]

Abstract: A hitherto unknown, atmospherically relevant, isotope-exchange reaction was studied in ionised gaseous mixtures containing carbon dioxide and monoxide. The mechanism of the O exchange, proceeding over a double-minimum potential-energy surface, was positively established by mass spectrometric and theoretical methods that also allowed the identification and characterisation of the $C_2O_3^+$ intermediate. The increase of internal energy displaces the observed reactivity towards an endothermic reaction path that involves only CO_2 and represents an indirect route to the dissociation of carbon dioxide.

Keywords: atmospheric chemistry · carbon oxides · density functional calculations · gas-phase reactions · mass spectrometry

Introduction

Although the importance of ionic processes in terrestrial and planetary atmospheres and the strong link with neutral chemistry have long been recognised,[1] the interest of atmospheric chemistry researchers in the reactivity of carbon oxides has concerned for the most part neutral species.[2]

As a part of our interest in ionic processes relevant to atmospheric chemistry,[3] we employed mass spectrometric techniques to study the reactivity observed in ionised mixtures containing CO_2 and CO, jointly present in several contexts of atmospheric relevance. The investigation, also implemented by theoretical calculations, disclosed an effective O-exchange process in the reaction of CO_2^+ with CO, and led to the detection and characterisation of the $C_2O_3^+$ intermediate. The obtained results have a bearing on the issue of isotopic enrichment of CO_2 and CO, observed in the atmospheres of Earth and Mars,[4] and are generally relevant to "charged" atmospheric environments where CO_2 and CO are present. Ion-neutral reactions are known to deeply affect the bulk composition of the tiny atmosphere of Mars, where CO_2^+ is one of the most abundant ions, and CO is counted among the major components.[5] Likewise, ionic processes occur in the Venusian atmosphere by lightning discharges in CO_2, providing high local concentrations of CO in a truly "charged" environment.[2]

Unlike Mars and Venus, where CO_2 is the major atmospheric component, the Earth's atmosphere contains only minor amounts of carbon dioxide, although it is one of the most important greenhouse gases. Such a difference has been traced to diverse evolution from the primitive atmospheric composition, that of the Earth being specifically aimed at sustaining life. However, the concentration and distribution of atmospheric gases can be changed as a result of human activities: the average increase of CO_2 levels from biomass burning, deforestation and industrial activities is evaluated to be about 3.3 $GtC\,year^{-1}$,[6] and the effects are more readily evident for less abundant components, such as carbon monoxide, which reaches high local concentrations in localised urban or industrial areas.[7] Thus progressive modifications of the carbon oxides budget might significantly affect the picture of ionic processes that occur in the Earth's lower atmosphere by galactic cosmic rays, UV radiation and lightning. Moreover, anthropogenic agents promote ionic processes that also involve excited species, for example, coronas along high-voltage power lines.

In summary, the observed reactivity will hopefully contribute to a more complete description of the reaction path-

[a] Prof. Dr. G. de Petris, Dr. A. Cartoni, Dr. A. Troiani
Dipartimento di Studi di Chimica e Tecnologia delle Sostanze Biologicamente Attive, Università "La Sapienza"
P.le Aldo Moro 5, 00185 Roma (Italy)
Fax: (+39) 06-49913602
E-mail: giulia.depetris@uniroma1.it

[b] Prof. Dr. M. Rosi
Dipartimento di Ingegneria Civile ed Ambientale
Sezione Tecnologie Chimiche e Materiali per l'Ingegneria
Università di Perugia
Via Duranti, 06131, Perugia (Italy)

[c] Dr. G. Angelini, Dr. O. Ursini
Istituto di Metodologie Chimiche
Area della Ricerca di Roma del CNR, CP 10
00016 Monterotondo Stazione (RM) (Italy)

 DOI: 10.1002/chem.200400483

ways relevant to atmospheric models and to a better understanding of those involving non-thermal or excited species.

Results

Formation of $C_2O_3^+$: Earlier mass spectrometric studies of CO_2 containing small amounts of CO identified the ligand-exchange reaction between $(CO_2)_2^+$ and CO as a route to $C_2O_3^+$.[8] On the basis of the literature available to date, CO_2^+ is apparently unreactive toward CO.[9] We re-examined the reaction between CO_2^+ and CO in ionised mixtures containing variable amounts of CO.

FT-ICR mass spectrometry: $^{13}CO_2^+$ ions were generated by electron impact in the first cell of a Fourier transform ion cyclotron resonance (FT-ICR) mass spectrometer. They were isolated by selective ejection techniques and, after a suitable "cooling" time of 1 s, they were transferred to the second cell and allowed to react with CO, at a pressure of $1–2\times10^{-7}$ Torr. The isotope exchange reaction given in Equation (1) was observed.

$$^{13}CO_2^+ + CO \rightarrow {}^{13}CO + CO_2^+ \quad (1)$$

The rate constant of this reaction at 298 K is $k_1 = 1.23 \pm 0.10\times10^{-10}\,cm^3s^{-1}molecule^{-1}$, which corresponds to a collisional efficiency k_f/k_{coll} of about 13%. Experiments performed with $C^{18}O_2^+$ and CO demonstrate that the CO_2^+ ions from reaction (1) undergo further isotope exchange. As shown in Figure 1, the initially formed $OC^{18}O^+$ ions react with CO eventually giving CO_2^+ [Eq. (2)].

$$C^{18}O_2^+ + CO \underset{a}{\rightarrow} (C^{18}O) + OC^{18}O^+ \xrightarrow[b]{+CO} (C^{18}O) + CO_2^+ \quad (2)$$

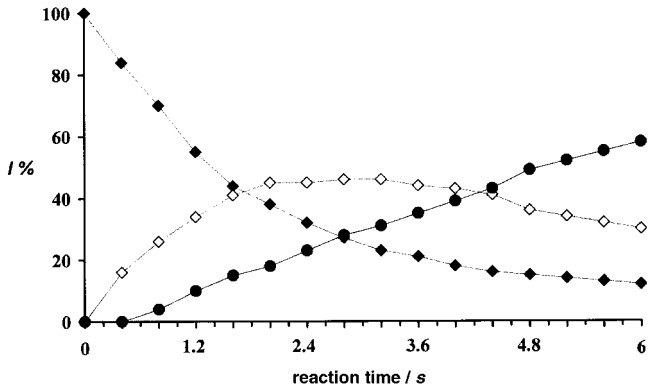

Figure 1. Time profile of the reaction of $C^{18}O_2^+$ with CO (■ $C^{18}O_2^+$, □ $C^{18}OO^+$, ● CO_2^+).

The measured rate constants, k_{2a} and k_{2b}, the latter obtained by reisolating the $OC^{18}O^+$ product ion, compare well with k_1. The occurrence of these reactions points to the formation of a transient $C_2O_3^+$ intermediate; however, this intermediate cannot be efficiently stabilised in the low-pressure regime typical of FT-ICR experiments. The same experiments were performed by isolation of CO^+, which exclusively undergoes charge transfer, a process efficiently occurring at the collision rate ($k = 10^{-9}\,cm^3s^{-1}molecule^{-1}$).[10]

CI mass spectrometry: In the high-pressure source of a multisector mass spectrometer, the $C_2O_3^+$ ions, likely intermediates of reaction (1), were stabilised and observed in the pressure range of 0.05–0.2 Torr. They were obtained by chemical ionisation (CI) of a CO_2/CO mixture, according to reaction (3):

Table 1. CI spectra of CO_2 and CO_2/CO mixtures.[a]

Mixture	CO_2^+	$C_2O_3^+$	Other peaks
	m/z(ion)I[%]		m/z(ion)I[%]
CO_2			
	44(CO_2^+)100	***72***($C_2O_3^+$)<1	*16*(O^+)1, *18*(H_2O^+)9, *19*(H_3O^+)2, *28*(CO^+)1,[b] *29*(COH^+)1,[c] *32*(O_2^+)9, *45*(CO_2H^+)8, *46*($CO\,H_2O^+$)2, *88*($(CO_2)_2^+$)1
P = 0.05 Torr	*44*(CO_2^+)100	***72***($C_2O_3^+$)<1	*16*(O^+)4, *18*(H_2O^+)10, *19*(H_3O^+)1, *28*(CO^+)6,[b] *29*(COH^+)<1,[c] *32*(O_2^+)5, *45*(CO_2H^+)9, *46*($CO\,H_2O^+$)2
CO_2/CO[d]			
HP CO	*44*(CO_2^+)100	***72***($C_2O_3^+$)1	*16*(O^+)2, *18*(H_2O^+)5, *19*(H_3O^+)6, *28*(CO^+)54, *29*(COH^+)29, *32*(O_2^+)3, *40*(C_2O^+)2, *45*(CO_2H^+)5, *46*($CO\,H_2O^+$)3, *56*($(CO)_2^+$)9, *57*($(CO)_2H^+$)<1, *68*($C_3O_2^+$)<1
HP CO_2	*44*(CO_2^+)100	***72***($C_2O_3^+$)1	*16*(O^+)1, *18*(H_2O^+)10, *19*(H_3O^+)2, *28*(CO^+)2, *29*(COH^+)4, *32*(O_2^+)11, *45*(CO_2H^+)8, *46*($CO\,H_2O^+$)2, *88*($(CO_2)_2^+$)2
CO_2/^{13}CO			
HP CO	*44*(CO_2^+)100	***73***($^{13}CCO_3^+$)1	*16*(O^+)3, *18*(H_2O^+)9, *19*(H_3O^+)35, *28*(CO^+, N_2^+)2,[b] *29*($^{13}CO^+$)28,
	45($^{13}CO_2^+$)59[e]	*74*($^{13}C_2O_3^+$)<1	*30*($^{13}COH^+$)70, *32*(O_2^+)14, *42*($^{13}C_2O^+$)1, *46*($CO\,H_2O^+$)4, *47*($^{13}CO\,H_2O^+$)6, *57*($CO\,^{13}CO^+$)2, *58*($(^{13}CO)_2^+$)14, *71*($^{13}C_3O_2^+$)<1
HP CO_2	*44*(CO_2^+)100	***73***($^{13}CCO_3^+$)1	*16*(O^+)1, *18*(H_2O^+)11, *19*(H_3O^+)8, *28*(CO^+)2,[b] *29*($^{13}CO^+$)3,
	45($^{13}CO_2^+$)11	*72*($C_2O_3^+$)<1	*30*($^{13}COH^+$)20, *32*(O_2^+)13, *46*($CO\,H_2O^+$)3, *47*($^{13}CO\,H_2O^+$)<1, *57*($CO^{13}CO^+$)1, *58*($(^{13}CO)_2^+$)2, *88*($(CO_2)_2^+$)1
$^{13}CO_2$/CO			
HP CO	*45*($^{13}CO_2^+$)100	***73***($^{13}CCO_3^+$)1	*16*(O^+)3, *18*(H_2O^+)7, *19*(H_3O^+)9, *28*(CO^+)29, *29*(COH^+)50, *30*($^{13}COH^+$)3,[c]
	44(CO_2^+)59	*72*($C_2O_3^+$)<1	*32*(O_2^+)9, *40*(C_2O^+)1, *46*($^{13}CO_2H^+$, $CO\,H_2O^+$)6, *47*($^{13}CO\,H_2O^+$)5, *56*($(CO)_2^+$)12, *57*($CO^{13}CO^+$)2, *68*($C_3O_2^+$)<1
HP CO_2	*45*($^{13}CO_2^+$)100	***73***($^{13}CCO_3^+$)1	*16*(O^+) 1, *18*(H_2O^+)12, *19*(H_3O^+)16, *28*(CO^+)5,
	44(CO_2^+)11	*74*($^{13}C_2O_3^+$)<1	*29*(COH^+)5, 30($^{13}COH^+$)2,[c] *32*(O_2^+)15, *46*($^{13}CO_2H^+$, $CO\,H_2O^+$)6, *47*($^{13}CO\,H_2O^+$)5, *56*($(CO)_2^+$)4, *57*($CO^{13}CO^+$)1, *90*($(^{13}CO_2)_2^+$)<1

Table 1. (Continued)

Mixture	CO_2^+ m/z(ion)I[%]	$C_2O_3^+$ m/z(ion)I[%]	Other peaks m/z(ion)I[%]
CO_2/$C^{18}O$			
HP CO	*44*(CO_2^+)100	***74***($C_2{}^{18}OO_2^+$)1	*16*(O^+)1, *18*(H_2O^+)9, *19*(H_3O^+)26, *20*($H_2{}^{18}O^+$)4, *21*($H_3{}^{18}O^+$)11, *28*(CO^+, N_2^+)3,[b]
	46($C^{18}OO^+$)61[f]	*76*($C_2{}^{18}O_2O^+$) < 1	*29*(COH^+)4,[c] *30*($C^{18}O^+$)41, *31*($C^{18}OH^+$)76, *32*(O_2^+)12, *34*($^{18}OO^+$)15, *36*($^{18}O_2^+$)3,
	48($C^{18}O_2^+$)34[f]	*78*($C_2{}^{18}O_3^+$) < 1	*42*($C_2{}^{18}O^+$)1, *45*(CO_2H^+)6, 47(4),[g] *58*(CO $C^{18}O^+$)3, *60*(($C^{18}O)_2^+$)14, *61*(($C^{18}O)_2H^+$)1
HP CO_2	*44*(CO_2^+)100	***74***($C_2{}^{18}OO_2^+$)1	*16*(O^+)2, *18*(H_2O^+)14, *19*(H_3O^+)11, *20*($H_2{}^{18}O^+$)2, *21*($H_3{}^{18}O^+$)1,
	46($C^{18}OO^+$)8[f]	*72*($C_2O_3^+$) < 1	*28*(CO^+)3,[b] *29*(COH^+)2,[c] *30*($C^{18}O^+$)4, *31*($C^{18}OH^+$)27, *32*(O_2^+)12,
	48($C^{18}O_2^+$)1[f]		*34*($^{18}OO^+$)4, *45*(CO_2H^+)8, 47(1),[g] *58*($COC^{18}O^+$)*1*, *60*(($C^{18}O)_2^+$)2, 88(($CO_2)_2^+$) < 1
$C^{18}O_2$/CO			
HP CO	*48*($C^{18}O_2^+$)100[f]	***76***($C_2{}^{18}O_2O^+$)1	*16*(O^+)2, *18*(H_2O^+)4, *19*(H_3O^+)24, *20*($H_2{}^{18}O^+$) < 1, *21*($H_3{}^{18}O^+$)5, *28*(CO^+)27,
	46($C^{18}OO^+$)61[f]	*74*($C_2{}^{18}OO_2^+$) < 1	*29*(COH^+)70, *30*($C^{18}O^+$)5,[b] *31*($C^{18}OH^+$)2,[c] *32*(O_2^+)14, *34*($^{18}OO^+$)15, *36*($^{18}O_2^+$)1,
	44(CO_2^+)32	*72*($C_2O_3^+$) < 1	*40*(C_2O^+) < 1, *45*(2),[g] 47(4),[g] *49*($C^{18}O_2H^+$)6, *56*(($CO)_2^+$)39, 57(($CO)_2H^+$)3,
			58($COC^{18}O^+$)6, *68*($C_3O_2^+$) < 1, *80*($C^{18}O_2O_2^+$) < 1
HP CO_2	*48*($C^{18}O_2^+$)100[f]	***76***($C_2{}^{18}O_2O^+$)1	*16*(O^+)1, *18*(H_2O^+)4, *19*(H_3O^+)7, *20*($H_2{}^{18}O^+$)1, *21*($H_3{}^{18}O^+$)3, *28*(CO^+)6,
	46($C^{18}OO^+$)15[f]	*78*($C_2{}^{18}O_3^+$) < 1	*29*(COH^+)27, *30*($C^{18}O^+$)3,[b] *31*($C^{18}OH^+$)1,[c] *32*(O_2^+)12,
	44(CO_2^+)3		*34*($^{18}OO^+$)6, 36($^{18}O_2^+$)5, 47(1)[g], *49*($C^{18}O_2H^+$)5,
			56(($CO)_2^+$)6, *58*($COC^{18}O^+$)2, 80($C^{18}O_2O_2^+$) < 1, 96(($CO_2)_2^+$) < 1
$C^{18}O_2$/^{13}CO			
HP CO	*48*($C^{18}O_2^+$)100[f]	***77***($^{13}CC^{18}O_2O^+$)1	*16*(O^+)5, *18*(H_2O^+)11, *19*(H_3O^+)24, *20*($H_2{}^{18}O^+$)3,
	47($^{13}C^{18}OO^+$)46[f]	*76*($^{13}C_2{}^{18}OO_2^+$) < 1	*21*($H_3{}^{18}O^+$)5, *28*(N_2^+)2, *29*($^{13}CO^+$)41, *30*($^{13}COH^+$)68,
	46($C^{18}OO^+$)10[f]	*74*($^{13}C_2O_3^+$) < 1	*31*($C^{18}OH^+$)4,[c] *32*(O_2^+)6, *34*($^{18}OO^+$)9, *36*($^{18}O_2^+$)2,
	49($^{13}C^{18}O_2^+$)7[h]		*42*($^{13}C_2O^+$)1, *58*(($^{13}CO)_2^+$)7, *59*($C^{18}O^{13}CO^+$)2,
	45($^{13}CO_2^+$)19		71($^{13}C_3O_2^+$) < 1
HP CO_2	*48*($C^{18}O_2^+$)100[f]	***77***($^{13}CC^{18}O_2O^+$)1	*16*(O^+)1, *18*(H_2O^+)15, *19*(H_3O^+)9, *20*($H_2{}^{18}O^+$)6,
	47($^{13}C^{18}OO^+$)5[f]	*78*($C_2{}^{18}O_3^+$) < 1	*21*($H_3{}^{18}O^+$)4, *28*(N_2^+)1, *29*($^{13}CO^+$)4, *30*($^{13}COH^+$)18,
	46($C^{18}OO^+$)5[f]		*31*($C^{18}OH^+$)2,[c] *32*(O_2^+)5, *34*($^{18}OO^+$)4, *36*($^{18}O_2^+$)11,
	49($^{13}C^{18}O_2^+$)9[h]		*58*(($^{13}CO)_2^+$)1, *59*($C^{18}O^{13}CO^+$)1, *96*(($CO_2)_2^+$) < 1
	45($^{13}CO_2^+$)1		
$^{13}CO_2$/$C^{18}O$			
HP CO	*45*($^{13}CO_2^+$)100	***75***($^{13}CC^{18}OO_2^+$)1	*16*(O^+) < 1, *18*(H_2O^+)13, *19*(H_3O^+)26, *20*($H_2{}^{18}O^+$)2,
	46($C^{18}OO^+$)51[f,i]	*76*($C_2{}^{18}O_2O^+$) < 1	*21*($H_3{}^{18}O^+$)5, *28*(N_2^+)2, *29*($^{13}CO^+$)3,[b] *30*($C^{18}O^+$)47,
	47($^{13}C^{18}OO^+$)10[f]		*31*($C^{18}OH^+$)60, *32*(O_2^+)7, *34*($^{18}OO^+$)7, *36*($^{18}O_2^+$)1,
	44(CO_2^+)10		42($C_2{}^{18}O^+$)1, *59*($C^{18}O^{13}CO^+$)1, 60(($C^{18}O)_2^+$)6,
	48($C^{18}O_2^+$)25[f]		72($C_3{}^{18}O_2^+$) < 1
HP CO_2	*45*($^{13}CO_2^+$)100	***75***($^{13}CC^{18}OO_2^+$)1	*16*(O^+)1, *18*(H_2O^+)19, *19*(H_3O^+)12, *20*($H_2{}^{18}O^+$) < 1,
	46($C^{18}OO^+$)13[f,i]	*74*($^{13}C_2O_3^+$) < 1	*28*(N_2^+) < 1, *29*($^{13}CO^+$)1,[b] *30*($C^{18}O^+$)2,
	47($^{13}C^{18}OO^+$)4[f]		*31*($C^{18}OH^+$)10, *32*(O_2^+)15, *34*($^{18}OO^+$)1,
	44(CO_2^+)4		*59*($C^{18}O^{13}CO^+$) < 1, *60*(($C^{18}O)_2)^+$) < 1, 90(($^{13}CO_2)_2^+$)1
	48($C^{18}O_2^+$) < 1[f]		

[a] Ions written in bold type are CO_2^+ ions from the O exchange and the investigated $C_2O_3^+$ ions. Unless stated otherwise, P = 0.1 Torr. HP CO_2, CO_2/CO ≈ 10; HP CO, CO/CO_2 ≈ 10. Unless stated otherwise, isobaric ions were identified by high-resolution CAD-TOF mass spectra. Ion abundances not exceeding 0.2% are not reported. [b] CO^+ from dissociation of CO_2^+. In mixtures containing unlabelled CO_2, at high CO pressure, N_2^+ is ≈70% of the peak abundance. [c] COH^+ from dissociation of CO_2H^+ (from MS/MS). [d] CI spectra of the unlabelled CO_2/CO mixture (P = 0.1 Torr), allowing us to exclude the formation of $(CO)_2H_2O^+$ and $CO_2CO(H)^+$ ions in all the investigated mixtures. [e] This peak contains 50% of CO_2H^+ at high CO_2 pressure and 10% at high CO pressure. Formation of m/z 73 from CO_2H^+ and CO is excluded on the basis of footnote [d] and on the absence of neutral CO in the mixture. The m/z 45 daughter ion from the CAD of $^{13}CCO_3^+$ is $^{13}CO_2^+$ (from MS/MS). [f] Peaks of m/z 46, 47 and 48 contain variable percentages, not exceeding 10%, of COH_2O^+ (m/z 46), $^{13}COH_2O^+$ (m/z 47) and $C^{18}OH_2O^+$ (m/z 48). Formation of $(CO)_2H_2O^+$ (m/z 74), $CO(H_2O)C^{18}O^+$ (m/z 76) and $^{13}CO(H_2O)C^{18}O^+$ (m/z 77), in those mixtures where peaks of m/z 74, 76 and 77 are the investigated adducts, is excluded based on footnote [d] and on high-resolution mass measurements. [g] $^{13}C^{18}OO^+$ and $C^{18}O^{17}O^+$ (m/z 47) and $^{13}CO_2^+$ (m/z 45) from the dissociation of isotopomers of the m/z 74 and m/z 76 adduct. Possible incursion of isotope effects should be investigated in addition to the role of repeated intra-complex isomerisation–fragmentation processes. [h] This peak contains variable amounts, not exceeding 60%, of $C^{18}O_2H^+$. Formation of m/z 78 from $C^{18}O_2H^+$ and ^{13}CO is excluded on the basis of footnote [d]. [i] This peak contains variable amounts, not exceeding 60%, of $^{13}CO_2H^+$. Formation of m/z 76 from $^{13}CO_2H^+$ and $C^{18}O$ is excluded on the basis of footnote [d].

$$CO_2^+ + CO \rightarrow C_2O_3^+ \quad (3)$$

and by CI of neat CO_2, probably from reaction (4).

$$CO_2^+ + CO_2 \rightarrow C_2O_3^+ + O \quad (4)$$

In CO_2/CO mixtures, the two reaction pathways were distinguished by utilising ^{13}C- and/or ^{18}O-labelled reactants. Labelled $C_2O_3^+$ ions, obtained exclusively by reaction (3), were detected utilizing the following CO_2/CO mixtures: 1) $^{13}CCO_3^+$ from either CO_2/^{13}CO or $^{13}CO_2$/CO, 2) $C_2{}^{18}OO_2^+$ from CO_2/$C^{18}O$, 3) $C_2{}^{18}O_2O^+$ from $C^{18}O_2$/CO, 4) $^{13}CC^{18}O_2O^+$ from $C^{18}O_2$/^{13}CO, 5) $^{13}CC^{18}OO_2^+$ from $^{13}CO_2$/$C^{18}O$. The CI spectra are reported in Table 1. The CO_2/CO mixtures were investigated at variable CO_2/CO ratios, namely at higher CO pressure (CO/CO_2 ≈ 10) and higher CO_2 pressure (CO_2/CO ≈ 10), respectively. In the latter case, the ligand exchange reaction between $(CO_2)_2^+$ and CO may also play a role in addition to reaction (3).[8] The unlabelled CO_2/CO mixture was first examined to monitor the CO^+ and CO_2^+ reactivity under the two experimental conditions investigated. All the experiments were then performed at the pressure

of 0.1 Torr, which minimises the formation of higher clusters.

Consistent with the FT-ICR results, the CI spectra show significant abundances of CO_2^+ ions from the O-exchange reactions, for example Reaction (5).

$$\underset{m/z\ 48}{C^{18}O_2^+} + CO \rightarrow \underset{m/z\ 76}{C_2{}^{18}O_2O^+} \rightarrow \underset{m/z\ 46}{{}^{18}OCO^+} + C^{18}O \quad (5)$$

The extent of the O exchange is significantly enhanced at high CO pressure (Figure 2A), which also allows subsequent reactions with the available neutral species [Reaction (6)].

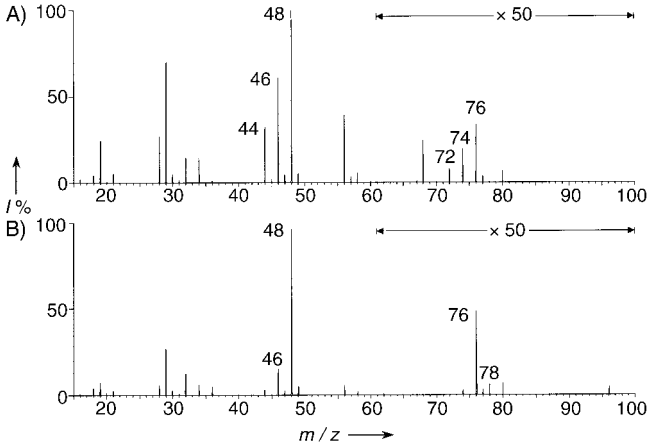

Figure 2. CI spectrum of the $C^{18}O_2$/CO mixture, A) high CO pressure and B) high CO_2 pressure. A) Note in addition to the $C_2{}^{18}O_2O^+$ adduct at *m*/*z* 76, the peaks at *m*/*z* 74 ($C_2{}^{18}OO_2^+$) and *m*/*z* 72 ($C_2O_3^+$). B) Note in addition to the $C_2{}^{18}O_2O^+$ adduct at *m*/*z* 76, a peak at *m*/*z* 78 ($C_2{}^{18}O_3^+$).

$$\underset{m/z\ 46}{{}^{18}OCO^+} + CO \rightarrow \underset{m/z\ 74}{C_2{}^{18}OO_2{}^+} \rightarrow \underset{m/z\ 44}{OCO^+} + C^{18}O \quad (6)$$

Two results stand out: firstly, the observed O exchange hints at a $C_2O_3^+$ intermediate having a O-C-O-C-O connectivity. Secondly, at high CO pressure, the high efficiency of the O exchange leads to CO_2^+ ions significantly enriched in the oxygen atom of carbon monoxide. Conversely, at higher CO_2 pressures, the minor efficiency of the O exchange accompanies formation of $C_2O_3^+$ isotopomers from the reaction pathway (4), also facilitated by the greater available amount of CO_2 (Figure 2B) [Reaction (7)].

$$\underset{m/z\ 48}{C^{18}O_2^+} + C^{18}O_2 \rightarrow \underset{m/z\ 78}{C_2{}^{18}O_3^+} + {}^{18}O \quad (7)$$

In addition to the analysis of isobaric species (Table 1), it is worth mentioning possible complications arising from the incursion of alternative formation processes. As an example, in $C^{18}O_2$/CO mixtures, an alternative route to the abovementioned $C_2{}^{18}O_2O^+$ ions could be envisaged in addition to Reaction (5), namely the reverse reaction between $^{18}OCO^+$ and $C^{18}O$. Such an alternative reaction channel deserves consideration, especially at high CO pressure, when the $^{18}OCO^+$ ion (*m*/*z* 46) is largely supplied in the source from Reaction (5). The accurate evaluation of the possible available amount of neutral $C^{18}O$ rules out this hypothesis. In all the examined mixtures, this type of contribution was carefully examined and ascertained to be ineffective, and the investigated $C_2O_3^+$ ions can be unambiguously traced to the reactants of the utilised CO_2/CO mixture.

On this basis, in each $C_2O_3^+$ ion, the CO_2 moiety traceable to the reactant will be hereafter referred to as the original CO_2^+. As an example, in $^{13}CCO_3^+$ ions obtained from a $^{13}CO_2$/CO mixture, $^{13}CO_2^+$ is the original CO_2^+, whereas in $^{13}CCO_3^+$ ions obtained from a $CO_2/^{13}CO$ mixture, CO_2^+ is the original CO_2^+.

TQ experiments: The effectiveness of Reaction (4) as a route to $C_2O_3^+$ was probed in experiments performed in a triple quadrupole (TQ) mass spectrometer (Figure 3A).

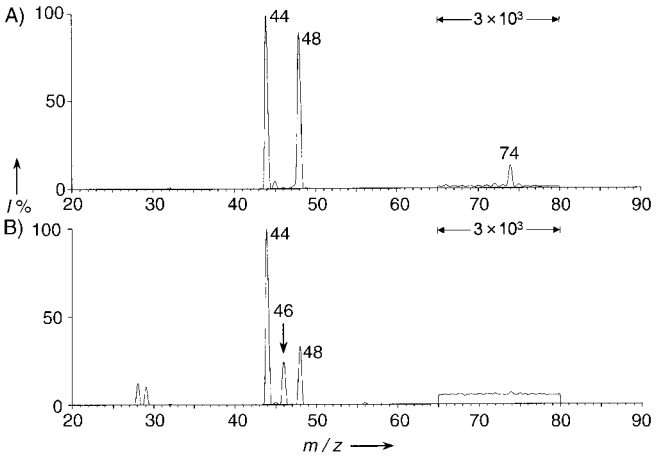

Figure 3. Mass spectrum of the charged products from the reaction of mass-selected $C^{18}O_2^+$ ions with A) CO_2 and B) CO.

CO_2^+ ions were generated in the external CI source, mass selected by the first quadrupole and allowed to react with CO_2 in the RF-only hexapolar cell at pressures ranging from 5×10^{-5} to 8×10^{-4} Torr. Adducts at *m*/*z* 72 ($C_2O_3^+$), 73 ($^{13}CCO_3^+$) and 74 ($C_2{}^{18}OO_2^+$) were observed from CO_2^+, $^{13}CO_2^+$ and $C^{18}O_2^+$, respectively. No peaks corresponding to the O-exchange process were observed. Moreover, the reactions of CO_2^+ with $C^{18}O_2$ [Reaction (8)] and of $C^{18}O_2^+$ with CO_2 [Reaction (9)], respectively, show that the oxygen atom is exclusively lost by CO_2^+.

$$CO_2^+ + C^{18}O_2 \rightarrow \underset{m/z\ 76}{C_2{}^{18}O_2O^+} + O \quad (8)$$

$$C^{18}O_2^+ + CO_2 \rightarrow \underset{m/z\ 74}{C_2{}^{18}OO_2{}^+} + {}^{18}O \quad (9)$$

The reactions of $C^{18}O_2^+$ and $^{13}CO_2^+$ with CO were also investigated. The results confirm the efficiency of the O exchange at high CO pressure, leading to depletion of the iso-

topic enrichment of CO_2^+, at the highest pressure investigated (Figure 3B). Only charge transfer was instead observed from the reaction of CO^+ with CO_2.

Structural analysis

MIKE-CAD mass spectrometry: The $C_2O_3^+$ ions (*m*/*z* 72) from Reactions (3) and (4) undergo unimolecular decomposition into CO_2^+ and CO^+ in the second field-free region of the mass spectrometer, in the 5×10^{-5} s time-window (Figure 4A). The resulting MIKE (mass-analyzed ion kinetic

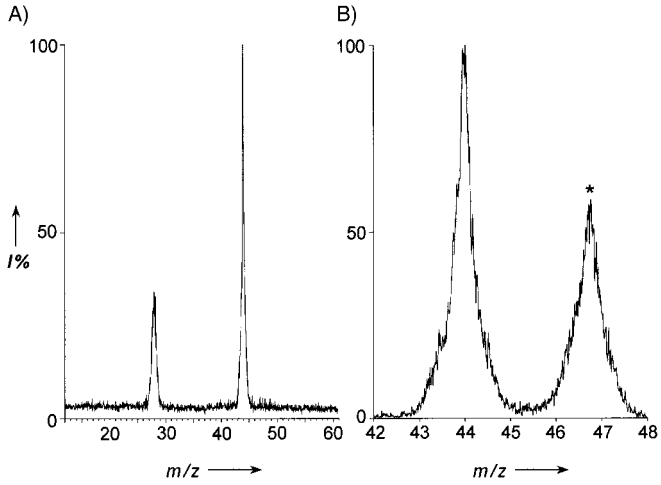

Figure 4. MIKE spectrum at high CO_2 pressure of A) $C_2O_3^+$ ions, B) *m*/*z* 44, * denotes the *m*/*z* 44 ionic fraction that decomposes within the collision cell, displaced at higher energies by application of a 1 keV voltage to the collision cell.

energy) spectrum shows an apparently composite peak at *m*/*z* 44 (CO_2^+), which reveals a collisional component when a keV additional voltage is applied to the collision cell (Figure 4B). A composite peak (where different shapes are superimposed) points to decompositions occurring over different transition states, as for example, those involving isomeric ions that decompose into the same fragment ion. However, ions having a high cross-section for collisional decomposition can display false composite peaks owing to residual gas in the collision cell region.[11] Thus on the basis of the shape analysis of the CO_2^+ peak, one would exclude that $C_2O_3^+$ ions of different structure are sampled. A deeper insight is given by the MIKE spectra of labelled $^*C_2{}^*O_3^+$ ions from Reaction (3) (Figure 5).

Spectra A–C in Figure 5 show the MIKE spectra recorded at high CO_2 pressure. As expected, they display peaks corresponding to the original CO_2^+ and the O-exchange product, that is, the $C_2{}^{18}O_2O^+$ ions obtained by CI of $C^{18}O_2$/CO display $C^{18}O_2^+$ and $OC^{18}O^+$ fragments [Figure 5C, Reactions (10) and (11)]:

$$C^{18}O_2^+ + CO \longrightarrow [C_2{}^{18}O_2O^+] \xrightarrow{m/z\ 48} C^{18}O_2^+ \quad (+CO) \qquad (10)$$

$$[C_2{}^{18}O_2O^+] \xrightarrow{m/z\ 46} OC^{18}O^+ \quad (+C^{18}O) \qquad (11)$$

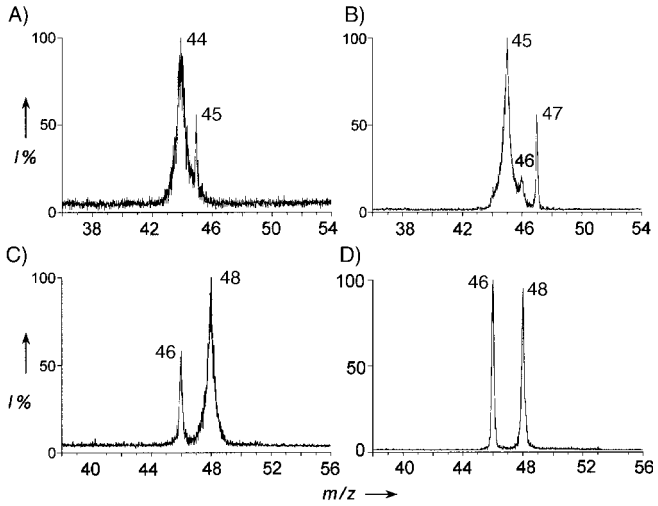

Figure 5. MIKE spectra of A) $^{13}CCO_3^+$ ions (*m*/*z* 73) from $CO_2/^{13}CO$ (ratio ≈10/1); B) $^{13}CCO_2{}^{18}O^+$ ions (*m*/*z* 75) from $^{13}CO_2/C^{18}O$ (ratio ≈10/1); C) $C_2{}^{18}O_2O^+$ ions (*m*/*z* 76) from $C^{18}O_2$/CO (ratio ≈10/1); D) $C_2{}^{18}O_2O^+$ ions (*m*/*z* 76) from $C^{18}O_2$/CO (ratio ≈1/10).

Interestingly, the two peaks show different widths and shapes. The peak at *m*/*z* 46 ($C^{18}OO^+$), corresponding to the product of the O exchange, exhibits features that are typical of loosely bound complexes: it is Gaussian-shaped and very narrow, and its kinetic energy release ($T_{0.5}$) amounts to only 9.5 meV. The wide collisional component, observed in CO_2^+ fragments from unlabelled $C_2O_3^+$ ions, is exclusively present in the original CO_2^+ (*m*/*z* 48), a circumstance met in all the labelled $C_2O_3^+$ ions. The peak does not have a clear-cut break in the slope, which prevents the analysis of the shape in comparison to that of the exchanged CO_2^+. Accordingly, it cannot be rigorously assessed whether or not the two decompositions occur over the same transition state. Nevertheless, labelling seems to effectively separate ionic fractions of different energy content that show different cross-sections for collisionally activated dissociation with low critical energy.[12] At high CO pressure, the MIKE picture is quite different: both peaks are narrow (Figure 5D), that corresponding to the original CO_2^+ still shows a residual broad component. Moreover, the fraction of $C_2O_3^+$ ions that decomposes unimolecularly ($\approx10^{-3}$) is greater than that at high CO_2 pressure ($\approx5\times10^{-5}$).

In summary, the overall evidence from the MIKE spectra marks a difference between the decomposition of the $C_2O_3^+$ ion into the original and the exchanged CO_2^+, and between the processes occurring at high CO_2 and high CO pressure, respectively. Finally, the intensities of the fragments are extremely variable, depending on even slight changes of the CO_2/CO ratio and of the total pressure in the source. However, at high CO_2 pressure, the abundance of the original CO_2^+ is reproducibly greater than that of the exchanged CO_2^+, at high CO pressure the CO^+ intensity is only about 1–2%.

The collisionally activated dissociation (CAD) spectra of the $C_2O_3^+$ ions, reported in Figure 6, essentially display the CO_2^+ and CO^+ fragments. The intensity of the CO_2^+ peaks increases on introduction of the collision gas into the cell

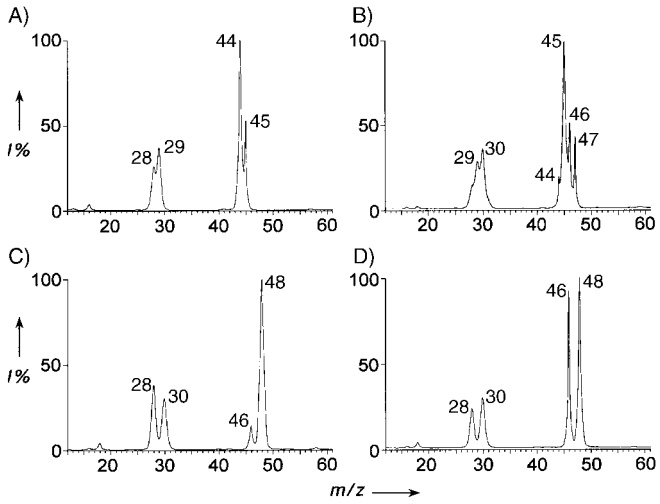

Figure 6. CAD spectra of $C_2O_3^+$ ions from different mixtures: A) $^{13}CCO_3^+$ ions (m/z 73) from $CO_2/^{13}CO$ (ratio ≈1/10); B) $^{13}CCO_2{}^{18}O^+$ ions (m/z 75) from $^{13}CO_2/C^{18}O$ (ratio ≈1/10); C) $C_2O^{18}O_2^+$ ions (m/z 76) from $C^{18}O_2/CO$ (ratio ≈10/1); D) $C_2O^{18}O_2^+$ ions (m/z 76) from $C^{18}O_2/CO$ (ratio ≈1/10).

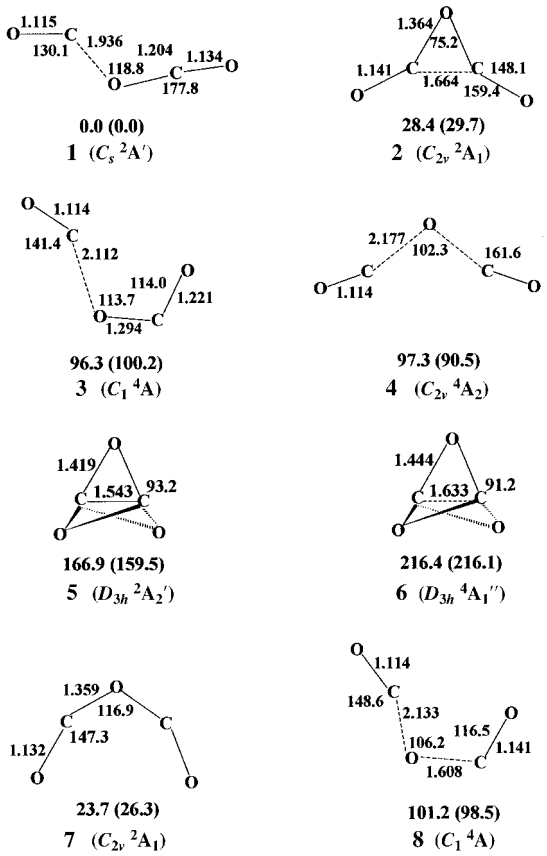

Figure 7. Optimised geometries of the stationary points localised on the potential-energy surface of $C_2O_3^+$, at the B3LYP level of theory. B3LYP (CCSD(T)) relative energies at 298 K are shown (bond lengths are in Å, angles in °, energies in kcal mol^{-1}).

and, consistent with the above, it increases by a factor of 100 at high CO_2 pressure, and by a factor of 30–40 at high CO pressure. Moreover, the CO_2^+ peaks are not Gaussian-shaped, particularly at high CO pressure where a narrower component is observed. Table 2 reports the abundances of the CO_2^+ fragments from labelled $C_2O_3^+$ ions. We found that the unimolecular contribution does not significantly affect the CAD fragmentation pattern. Nonetheless, given the scarce reproducibility of the MIKE pattern, the abundances have been corrected for such a contribution, evaluated by recording MIKE and CAD spectra in each experiment (see the Experimental Section). The ratio between the original CO_2^+ fragment and the O-exchanged CO_2^+ is fairly reproducible under the two experimental conditions investigated ($CO/CO_2 \approx 10$ and $CO_2/CO \approx 10$), and is always greater at high CO_2 pressure. Interestingly, the CAD spectra of ^{13}C- and ^{18}O-labelled reactants (Figure 6B) display all the possible combinations of labelled CO_2^+ fragment ions, with a predominance of the original CO_2^+ ($C^{18}O_2^+$, $^{13}CO_2^+$).

Table 2. Intensities (% Σ) of CO_2^+ fragments in the CAD spectra of labelled $C_2O_3^+$ ions.[a]

Parent ions (Mixture)		Fragments CO_2^+ (m/z 44)	$^{13}CO_2^+$ (m/z 45)	$C^{18}OO^+$ (m/z 46)	$^{13}C^{18}OO^+$ (m/z 47)	$C^{18}O_2^+$ (m/z 48)	$^{13}C^{18}O_2^+$ (m/z 49)
$^{13}CCO_3^+$	S[b]	50	50				
($CO_2/^{13}CO$)	A[c]	**61**	39				
	B[c]	**83**	17				
$^{13}CCO_3^+$	S	50	50				
($^{13}CO_2/CO$)	A	34	**66**				
	B	16	**84**				
$C_2{}^{18}O_2O^+$	S			67		33	
($C^{18}O_2/CO$)	A			48		**52**	
	B			12		**88**	
$C_2{}^{18}OO_2^+$	S	33		67			
($CO_2/C^{18}O$)	A	**52**		48			
	B	**87**		13			
$^{13}CC^{18}O_2O^+$	S			33	33	17	17
($C^{18}O_2/^{13}CO$)	A			21	28	**40**	11
	B			9	20	**64**	7
$^{13}CC^{18}OO_2^+$	S	17	17	33	33		
($^{13}CO_2/C^{18}O$)	A	13	**44**	25	18		
	B	8	**71**	15	6		

[a] Intensities derived by applying a 1 keV voltage to the collision cell, see the Experimental Section. [b] S = expected from randomisation. [c] A = High CO pressure, B = High CO_2 pressure, the original CO_2^+ intensities are in bold.

Theoretical results: Figure 7 shows the optimised geometries of the species identified on the doublet and quartet surface of $C_2O_3^+$. The $C_s{}^2$A′ doublet **1** is the most stable ion, 33.2 and 27.4 kcal mol^{-1} more stable than the dissociation products, CO_2^+ and CO, at the B3LYP and CCSD(T) levels, respectively. The $C_{2v}{}^2$A$_1$ ion **2** is not a true minimum at the CCSD(T) level, as it is unstable towards dissociation once the zero-point energy correction is included. At higher energies, we localised two quartet ions, the $C_1{}^4$A ion **3** and the $C_{2v}{}^4$A$_2$ ion **4**. At much

higher energies, the doublet and quartet ions **5** and **6** were found, which have highly strained, propellane-like structures. Species **7** and **8** are saddle points, and correspond to the transition states for the O-exchange reaction of ion **1**, and for **3**→**4** isomerisation, respectively. The kinetic barrier for O exchange from ion **1** was computed to amount to 23.7 and 26.3 kcal mol^{-1}, at the B3LYP and CCSD(T) levels of theory, respectively. The barrier for the **3**→**4** isomerisation, leading to O exchange from the quartet ion **3**, was computed to amount to 4.9 kcal mol^{-1} at the B3LYP level of theory, whereas no barrier was found at CCSD(T) level.

Discussion

The isotopic exchange reaction: The experimental evidence demonstrates that the O-exchange reaction is a rather efficient process, proceeding through the intermediacy of a stable $C_2O_3^+$ ion of OCOCO connectivity. The $C_2O_3^+$ intermediate, not detectable in FT-ICR experiments, can be effectively stabilised and detected under chemical ionisation conditions, which allows its structural analysis. The most salient result stands out in the structural assay of $C_2O_3^+$.

The CAD spectrum of the most simple $^{13}CCO_3^+$ system (Figure 6A) shows that the abundance of the CO_2^+ and $^{13}CO_2^+$ fragments is not comparable, as one would expect from the dissociation of a $C_2O_3^+$ ion of OCO^{13}CO structure. In contrast, the peak corresponding to the original CO_2^+ is greater than that of the exchanged CO_2^+, and their ratio increases at high CO_2 pressures. Likewise in $C_2{}^{18}O_2O^+$ ions of Figure 6D, the 1:1 ratio between the original CO_2^+ and the exchanged CO_2^+ becomes approximately 10:1 at high CO_2 pressure (Figure 6C). All the evidence from the structural analysis suggests the presence of ions that do not undergo the O-exchange process, particularly at high CO_2 pressure. A workable hypothesis could be the formation of ions of OC–CO_2 connectivity, not viable to the O exchange, which decompose exclusively to the original CO_2^+. However, no minimum having the OC–CO_2 connectivity was found by the theoretical analysis on the potential energy surface of $C_2O_3^+$, in agreement with previous results.[13]

According to theory, the stable minima of OCOCO connectivity are ions **1**, **3** and **4** (Figure 7). Formation of the quartet ions **3** and **4** is very unlikely under CI conditions because it would require quartet states of the CO_2^+ reactant ions, which are not sufficiently long-lived to undergo reaction (3).[14] The only $C_2O_3^+$ ion of OCOCO connectivity realistically formed is ion **1**, best described as an electrostatic $[CO_2{-}{-}{-}{*}CO]^+$ complex. Theory and experiment thus work together to discard the possibility that the O exchange is mediated by a symmetrical $C_2O_3^+$ ion. To gain a deeper insight into the process, we probed $C_2O_3^+$ ions of different energy contents and lifetimes in the different time windows available to observation in the mass spectrometer.

The mechanism: The metastable ions populate a narrow energy range (<1 eV) above the dissociation threshold and decompose spontaneously in the 5×10^{-5} s timeframe. They are hence very informative of the kinetics of the process. As illustrated in the previous section, it cannot be positively established if the dissociations into the original and exchanged CO_2^+ occur via different transition states. However, we exclude that the $[CO_2{-}{-}{-}{*}CO]^+$ ion **1** directly dissociates, over different transition states, into the original and the exchanged CO_2^+. Indeed, the expected barrier for the O exchange would result in a larger kinetic energy release than that associated with dissociation into the original CO_2^+. Conversely, the observed differences between the two processes are more consistent with $C_2O_3^+$ ions that dissociate over the same transition state with different energy contents, as for instance, ions that have been formed directly or following isomerisation. Labelling clearly indicates that only those $C_2O_3^+$ ions which decompose into the original CO_2^+, and hence formed directly from Reaction (3), have a high cross-section for CAD. Accordingly, the exchanged CO_2^+ fragment could be traced to dissociation of a rearranged ion **1**, only differing in the location of the oxygen atoms within the CO_2 and CO moieties [Eq. (12)].

$$CO_2^+ \longleftarrow \underset{\mathbf{1}}{[OCO\text{---}{*}CO]^+} \longrightarrow \underset{\mathbf{1a}}{[OC\text{---}O{*}CO]^+} \longrightarrow {}^{*}CO_2^+ \qquad (12)$$

Labelling thus separates these two populations to unravel an otherwise undetectable complex **1a**, $[CO{-}{-}{-}{*}CO_2]^+$, and builds up a convincing case for a process occurring through isomerisation of the formerly formed adduct **1** to a similar ion **1a**. Both are asymmetrical $C_2O_3^+$ ions, expected to dissociate into the original and the O-exchanged CO_2^+, respectively.

Consistent with this reasoning, the different energy of the decomposing ions **1** and **1a** depends on the energetic details of the potential energy surface. Particularly telling evidence is given by the small kinetic energy release associated with the fragmentation of the isomerised ion **1a** into the exchanged CO_2^+. This result decidedly argues for a barrier to the isomerisation not higher than or comparable to the dissociation limit. Accordingly, ions **1a**, formed in the source with a low energy excess or following isomerisation of **1** in the metastable time window,[15] undergo a near-threshold dissociation to give the narrow peak, typical of loosely bound complexes.

On the whole, the mutually supporting evidence shows that 1) the sampled $C_2O_3^+$ ions decompose into the original and the exchanged CO_2^+, by direct dissociation and through isomerisation to a similar $C_2O_3^+$ complex, respectively, 2) the barrier to isomerisation is comparable to the dissociation threshold.

The theoretical investigation agrees with the suggested mechanism. Indeed, we found that the saddle point for the isomerisation of ion **1** to the twin ion **1a** is located slightly below the dissociation limit, and O exchange occurs through the double-well surface depicted in Figure 8. It is known that processes having very close activation energies for dissociation and isomerisation are significantly governed by the different geometries of the transition states that favour the back dissociation with respect to the isomerisation, where loss in rotational entropy is greater.[16] As a consequence,

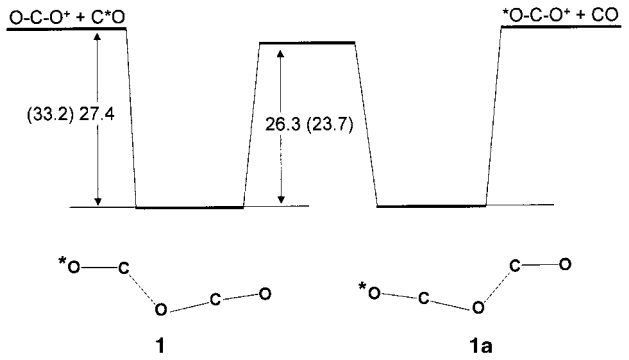

Figure 8. Energy profile ($\Delta H^{\ominus}$, kcal mol^{-1}) relevant to the reaction of C*OO$^+$ with CO. The CCSD(T) (B3LYP) energies are reported.

there is no complete equilibration prior to dissociation. Moreover, the k_{diss} is expected to be much greater than k_{isom} at higher internal energies, since tight transition states (isomerisation processes) display a shallower rise of k with E with respect to loose transition states (simple bond cleavage). On this ground, the MIKE evidence, showing a more effective competition between k_{diss} and k_{isom} at high CO_2 pressure, would indicate that a higher energy content characterise the $C_2O_3^+$ ions that decompose under these conditions in 5×10^{-5} s. Conversely, the narrow peaks observed at high CO pressure, for both the original and exchanged CO_2^+, hint at isomerisation–dissociation processes from lower energy ions, also consistent with the lower intensity of the CO^+ fragment and the more abundant metastable fragmentation observed under these conditions ($\approx10^{-3}$ with respect to $\approx10^{-5}$ at high CO_2 pressure).[17]

On this basis, depending on the experimental conditions, different amounts of ions **1** and **1a** can be expected to make up the stable $C_2O_3^+$ ionic population. Unlike metastable ions, these $C_2O_3^+$ ions do not spontaneously decompose and can be structurally analysed in their potential wells by CAD. At first glance, the structural analysis would thus suggest that the $C_2O_3^+$ population largely consists of ions **1**. The examination of the most and the least energetic fractions of $C_2O_3^+$ ions contributes to a better understanding of the whole process.

The $C_2O_3^+$ ion: The O exchange observed in the source, from the most energetic and short-lived $C_2O_3^+$ ions, is quite consistent with the picture outlined by the long-lived metastable fraction. It is clearly apparent that the O exchange is a significant process at high CO pressure, and becomes considerably minor at higher CO_2 pressure (Figure 2, Table 1). However, the whole process in the source is intricately affected by the energy of the reactant ions, the formation process, the thermalising ability of the bulk gas and competing reactions. Moreover, the identification of the most energetic conditions in the source is hardly conclusive.

Actually, a more "cooled" CO_2^+ population is expected at high CO pressure, when a considerable ionic fraction is formed with no energy excess by the low exothermic (5.3 kcal mol^{-1}) charge transfer from CO^+.[18] On the other hand, at high CO_2 pressure, the $C_2O_3^+$ ions could be more effectively thermalised, below both the barriers to dissociation and isomerisation, by the bulk gas CO_2. On the whole, the greater extent of the O exchange observed in the source at high CO pressure hints at a more effective **1**→**1a** isomerisation, and accordingly a major fraction of the **1a** ions is expected to be prepared, under these conditions, within the stable $C_2O_3^+$ population.

Such an inference is well confirmed by the analysis of the stable $C_2O_3^+$ ions, which live 5×10^{-5} s without decomposing. They are sampled by CAD below the dissociation threshold and are therefore structurally informative, unravelling even more interesting aspects, such as the extensive isotopic scrambling in $^{13}CC^{18}O_2O^+$ and $^{13}CC^{18}OO_2^+$ ions.

Considering, for example, the **1** and **1a** adducts formed by CI of a $C^{18}O_2/^{13}CO$ mixture, one would expect $C^{18}O_2^+$ (m/z 48) and $^{13}CO^{18}O^+$ (m/z 47) to be the fragmentation products, whereas peaks corresponding to $^{13}C^{18}O_2^+$ (m/z 49) and $CO^{18}O^+$ (m/z 46) are also observed. Based on theory, the doublet (**5**) and quartet ions (**6**) are viable to dissociation into the observed fragments; however, their formation in the source is very unlikely on account of their very high energy, and moreover their fragmentation products would be characterised by a large kinetic energy release. The observed fragmentation thus points to a scrambling occurring within the **1** and **1a** complexes through repeated rotations and consecutive isomerisations, as illustrated in Scheme 1.

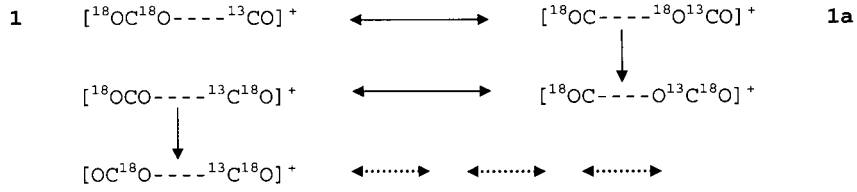

Scheme 1.

This process, whose prerequisite is the first isomerisation to **1a**, does not result in a fully randomised population. The distribution of the fragments expected from randomisation of all the labelled $C_2O_3^+$ ions is reported in Table 2. Three main groups can be identified based on the statistical distribution of the fragment: 1) $^{13}CCO_3^+$ ions formed from ^{13}C-labelled reactants (1:1 original/exchanged), 2) $C_2{}^{18}OO_2^+$ and $C_2{}^{18}O_2O^+$ ions formed from ^{18}O-labelled reactants (1:2 original/exchanged) and 3) $^{13}CC^{18}O_2O^+$ and $^{13}CC^{18}OO_2^+$ ions formed from $^{13}C/^{18}O$-labelled reactants (1:5 original/exchanged). As anticipated, the largest variation is observed in the original CO_2^+, the reliable signature of ions **1**. On the whole, the structural analysis confirms that, in all the systems and experimental conditions investigated, the $C_2O_3^+$ population, prepared and cooled in the source in the energy range below the dissociation threshold, contains a major amount of ions **1** with respect to ions **1a**, and ions **1** are even more significantly captured at high CO_2 pressure.

Finally, it is worth considering that the ions sampled by CAD possess a broad range of internal energies, including a higher-energy fraction that is below the dissociation threshold but above the isomerisation barrier. These ions are not sufficiently "hot" to decompose in the metastable window, but still susceptible to undergoing isomerisation during the flight, giving a mixture of interconverting structures that, in the absence of collisional relaxation, are not thoroughly randomised. The signature of these ions is found in particular at high CO pressure, where the CAD peaks show residual narrow components. The shape analysis and the evaluation of the metastable contribution indicate that these components are not due to the overlapping of metastable peaks,[11] whereas they are more probably attributable to the prompt dissociation by collision of these "stable" vibrationally excited ions that are already close to the dissociation limit.[12a,19] Accordingly, at high CO_2 pressure, lower-energy ions are sampled below the dissociation threshold and below the isomerisation barrier.

A high-energy route to $C_2O_3^+$: CI and TQ experiments provided evidence for a high-energy reaction pathway to $C_2O_3^+$ ions: the reaction of CO_2^+ with CO_2 [Eq. (4)]. We computed the $\Delta H^\ominus$ of the process, amounting to 95.8 and 90.0 kcal mol^{-1}, at the B3LYP and CCSD(T) levels of theory, respectively. The occurrence of Reaction (4) in ionised CO_2 thus hints at the presence of highly vibrationally excited CO_2^+ reactant ions.

In CO_2/CO mixtures, the $C_2O_3^+$ ions from Reaction (4) can be identified by isotopic labelling that separates the $C_2O_3^+$ ions from Reaction (3). They are detectable at high CO_2 pressure (Figure 2B), when actually excited CO_2^+ ions are probably formed by electron impact on CO_2. However, their formation from Reaction (4) is not straightforward. Indeed, the same product could be formed by ligand-exchange reaction between the ion **1a** and the available CO_2 [Reaction (13)].

$$C^{18}O_2^+ + CO \longrightarrow \underset{\mathbf{1}}{[^{18}OC^{18}O\text{--}CO]^+} \longrightarrow \underset{\mathbf{1a}}{[^{18}OC\text{--}^{18}OCO]^+} \xrightarrow{+\,C^{18}O_2} [^{18}OC\text{--}^{18}OC^{18}O]^+ \qquad (13)$$

This process is expected to be less favoured with respect to the competitive formation of $[^{18}OC{-}{-}{-}CO]^+$, which is even observed in the presence of small amounts of CO,[8] yet it could play a role at higher CO_2 pressure. Nonetheless, even not considering formation of this $C_2O_3^+$ isotopomer as a signature of the occurrence of Reaction (4) in CO_2/CO mixtures, its formation in neat CO_2 undoubtedly points to the presence of CO_2^+ ions having the required, albeit high, amount of energy. Low-lying electronic states of CO_2^+ are very short-lived owing to radiative decay or predissociation; however, their participation in the formation of ground state CO_2^+ ions having large amounts of internal energy has been considered, for example, in intersystem crossing associated with the predissociation of state C.[14a]

The fate of the $C_2O_3^+$ ions formed by Reaction (4) is necessarily related to their energy. As a matter of fact, it is difficult to evaluate the amount of energy available to species generated from excited reactant ions of unpredictable energy content. In principle, we can guess that, if sufficiently thermalised or formed by a slightly exothermic reaction, they do not undergo any O-exchange reaction. In contrast, if formed by a very exothermic process, they decompose into CO_2^+ and CO, favouring back-dissociation with respect to isomerisation. Both hypotheses could be valid, for instance, in our TQ experiments, showing no peaks but the original CO_2^+.

The loss of the oxygen atom from the CO_2^+ reactant ion suggests that, when the back-dissociation of the $C_2O_3^+$ product is favoured, the whole process is a dissociative charge transfer to CO_2 [Reactions (14)–(16)].

$$CO_2^+ + C^*O_2 \longrightarrow C_2{}^*O_2O^+ + O \qquad (14)$$

$$C_2{}^*O_2O^+ \longrightarrow C^*O_2^+ + CO \qquad (15)$$

$$CO_2^+ + C^*O_2 \longrightarrow C^*O_2^+ + CO + O \qquad (16)$$

In CO_2 plasmas, where CO_2^+ and CO_2 have the same isotopic composition, the net reaction is essentially the dissociation of CO_2 into CO and O.

Atmospheric implications: Ion-catalysed reactions are widely recognised as a class of important processes affecting the neutral composition of the stratosphere and troposphere, where ionisation occurs by galactic cosmic rays and UV radiations.[1–2] The O-exchange reaction, although not affecting the carbon dioxide and carbon monoxide budgets, can act on environments in which CO_2 and CO have *different* isotopic enrichments. Stratospheric and tropospheric CO_2 is, for example, enriched in both ^{17}O and ^{18}O. In particular, the tropospheric isotope values are very different from stratospheric values and they reflect mass-independent isotope effects.[4,20] The observed O exchange can modify the isotope distribution of CO_2^+ and CO by subsequent sequestering of oxygen atoms in carbon monoxide (Figure 2B, Figure 3B). This ionic route can be also of interest to the Martian atmosphere, where ^{17}O enrichment has been observed in Martian meteorites, from CO_2 transfer to carbonate minerals.[21] Here the CO_2^+ ion density reaches 10^4 cm^{-3},[5a] and O_2 is present in far minor amounts with respect to Earth. The evolution of the global process in the Martian atmosphere is not yet fully understood, and unrecognised sinks of ^{17}O have been suggested. Interestingly, one of the targets of the current missions to Mars is the measurement of the isotope ratios of CO_2, H_2O and noble gases, to hopefully provide a deeper insight into the evolution of the Martian atmosphere.

It is also worth considering that several atmospheric environments are far from equilibrium. Transient events, such as lightning, coronas along high-voltage power lines or during thunderstorms, typically ensure high local densities of vibrationally or electronically excited species whose role in promoting endothermic reactions is widely recognised.[22] The failure of equilibrium treatment to describe and interpret

some atmospheric phenomena has heightened the awareness that atmospheric models should make allowances for reactions of excited species. In this connection, a "high-energy" route to O exchange can be envisaged from the symmetrical quartet ion **3**, accessible from the long-lived CO ($^3\prod_r$). The most interesting outcome from high-energy CO_2^+ ions is the catalysed dissociation of carbon dioxide through Reaction (4), an endothermic process that is, however, less energetically demanding than dissociation of CO_2^+ into either O^+ or CO^+.[14a] Such process could be relevant as a local source of CO along high-voltage power lines, especially near urban or industrial areas where CO_2 production is more extensive. Furthermore, the process could be very effective in the ionospheres of Mars and Venus, where the bulk gas is itself CO_2. In this connection, it has already been observed that lightning discharges in Venus, a good example of a charged, non-equilibrated system, are an effective local source of carbon monoxide.[2]

Conclusion

In ionised CO_2/CO mixtures, a rather effective O exchange is undergone by thermal CO_2^+ ions via a $C_2O_3^+$ ion of OCOCO connectivity. The reaction efficiency is critically affected by the internal energy deposited into the initially formed $C_2O_3^+$ adduct, whose decomposition is favoured with respect to O exchange, occurring through a double-minimum potential-energy surface. Under highly energetic conditions, an indirect, ulterior route to dissociation of carbon dioxide into CO and oxygen atom is provided by the reaction of excited CO_2^+ ions with CO_2.

Experimental Section

FT-ICR experiments: The FT-ICR experiments were performed in an Extrel FTMS 2001 double-cell mass spectrometer equipped with an IonSpec Data Station and a FTMS Autoprobe. The ions were generated in the first cell and transferred into the second cell, where they were isolated by broad-band ejection pulses and by the Arbitrary Form method, after a cooling period of 1 s. Then they were allowed to react with neutral CO admitted into the cell in order to reach a stationary pressure of $1-2\times10^{-7}$ Torr. The pseudo-first-order rate constant was obtained from the slope of the logarithmic plot of the relative ion intensity versus the reaction time. The number density of the neutral molecules was calculated from the readings of the Bayard–Alpert gauge, corrected according to a standard procedure based on the correlation between relative sensitivity and the polarisability of the gas.[23] The efficiency of the reaction was expressed as the ratio of its bimolecular rate constant to the collision rate constant, calculated according to the ADO theory, or by the Su and Chesnavich parametrised variational theory,[24] that gave very similar results.

CI-MIKE-CAD experiments: The experiments were performed on a modified ZABSpec oa-TOF instrument (VG Micromass) with a EBE-TOF configuration, where E and B stand for electric and magnetic sectors, respectively, and TOF for orthogonal time-of-flight mass spectrometer. The instrument was fitted with an EI/CI source, a gas cell located in the first field free region and two pairs of gas cells located after the magnet along the beam path. Typical operating conditions of the CI source were as follows: accelerating voltage: 8 keV, source temperature: 423 K, repeller voltage: 0 V, emission current 1 mA, nominal electron energy: 50 eV. The source pressure was measured inside the source block by a Magnehelic differential pressure gauge. The gases were introduced into the source by separate inlets. Water amounts of $\approx10\,\%$ were still present following purging and heating of lines, owing to water desorbed from the glass vessels containing the labelled samples.

The MIKE and CAD spectra were recorded at 8 keV and with fully open source and energy slits. The MIKE spectra were averaged over 100 acquisitions to improve the signal-to-noise ratio. On account of the poor signal, the kinetic energy release was measured on resolved peaks at an energy resolution of 4000. The target gas utilised in the CAD experiments was He, admitted into the first cell at such a pressure to achieve a 70 % transmittance. The CAD abundances were derived from the peak heights, and the error from the overlap in $^{13}C/^{18}O$-labelled ions could lead to an overestimate of the randomised population. The CAD abundances were corrected by applying a keV voltage to the collision cell, which allows discrimination against all fragmentation occurring outside the cell. The same procedure was followed in the corresponding MIKE spectrum, which allows evaluation of the residual contribution from the ions that decompose unimolecularly within the cell. Although the results are best used with caution, the metastable component can be overestimated, if anything, owing to possible collisions with the gas near the cell (it has been generally evaluated to be $<1\,\%$ at high CO_2 pressure and, at most, 2.5 % at high CO pressure). The shape of the CAD peaks was analysed at an energy resolution of 5500, on resolved peaks corresponding to the original and O-exchange CO_2^+ fragments. High-resolution CAD-TOF experiments were performed to identify isobaric species in the investigated CI plasmas. The ions of interest, separated, mass-selected and accelerated to 8 keV, were transmitted to the TOF sector and structurally analysed by introducing He into the gas cell.

CO_2 and CO, were research-grade products with a stated purity in excess of 99.95 mol %. The $C^{18}O$ (98.8 ^{18}O atom %), ^{13}CO (99.0 ^{13}C atom %), $^{13}CO_2$ (99.0 ^{13}C atom %) and $C^{18}O_2$ (98.7 ^{18}O atom %) samples were obtained from Icon Stable Isotopes, Inc.

TQ experiments: The experiments were performed with a Waters Quattro Micro Tandem GC-MS/MS equipped with a cool chemical ionisation source. The ions generated in the source were mass-selected in the first quadrupole (Q1) and driven to the second quadrupole (Q2), a RF-only hexapole, containing the neutral gas at pressures ranging from 5×10^{-4} to 1×10^{-3} Torr. The ion–molecule reactions were investigated at a nominal collision energy of 0 eV and the charged products were analysed with the third quadrupole (Q3).

Computational methods: Density functional theory, with the hybrid[25] B3LYP functional,[26] was used to localise the stationary points of the investigated systems and to evaluate the vibrational frequencies. Although it is well known that density functional methods using non-hybrid functionals sometimes tend to overestimate bond lengths,[27] hybrid functionals, such as B3LYP, usually provide geometrical parameters in excellent agreement with experiment.[28] Single-point energy calculations at the optimised geometries were performed with the coupled-cluster single and double excitation method[29] with a perturbational estimate of the triple excitation [CCSD(T)] approach,[30] to include extensively correlation contributions.[31] Transition states were located with the synchronous transit-guided quasi-Newton method developed by Schlegel and co-workers.[32] The 6-311+G(3d) basis set was used.[33] Zero-point energy corrections, evaluated at the B3LYP/6–311+G(3d) level, were added to the CCSD(T) energies. The 0 K total energies of the species of interest were corrected to 298 K by adding translational, rotational and vibrational contributions. The absolute entropies were calculated by standard statistical-mechanistic procedures from scaled harmonic frequencies and moments of inertia relative to B3LYP/6–311+G(3d) optimised geometries. All calculations were performed with Gaussian 03.[34]

Acknowledgement

Financial support by the Italian Government (COFIN-FIRB), Rome University "La Sapienza" and CNR-MIUR (Legge 16–10–2000 Fondo FISR) is gratefully acknowledged.

[1] a) E. E. Ferguson, F. C. Fehsenfeld, D. L. Albritton, *Gas phase ion chemistry*, Academic Press, San Diego, **1979**; b) D. Smith, P. Spanel, *Mass Spectrom. Rev.* **1995**, *14*, 255; c) S. H. Seinfeld, S. N. Pandis, *Atmospheric chemistry and physics*, Wiley, Chichester, **1998**; d) R. S. MacTaylor, A. W. Castleman, Jr., *J. Atmos. Chem.* **2000**, *36*, 23.

[2] R. P. Wayne, *Chemistry of Atmospheres*, Clarendon Press, Oxford, **2000**.

[3] G. de Petris, *Mass Spectrom. Rev.* **2003**, *22*, 251.

[4] M. H. Thiemens, *Science* **1999**, *283*, 341.

[5] a) W. B. Hanson, S. Santini, D. R. Zuccaro, *J. Geophys. Res.* **1977**, *82*, 4351; b) E. Lellouch, G. Paubert, T. Encrenaz, *Planet. Space Sci.* **1991**, *39*, 219; c) V. A. Krasnopolsky, *J. Geophys. Res. [Atmos.]* **2003**, *108*, 5010.

[6] G. P. Brasseur, J. J. Orlando, G. S. Tyndall, *Atmospheric Chemistry and Global Change*, Oxford University Press, Oxford, **1999**.

[7] P. J. Crutzen, P. H. Zimmermann, *Tellus* **1991**, *43AB*, 136.

[8] a) L. W. Sieck, R. Gorden, P. Ausloos, *Planet. Space Sci.* **1973**, *21*, 2039; b) L. W. Sieck, *Int. J. Chem. Kinet.* **1978**, *10*, 336.

[9] a) S. Jaffe, F. S. Klein, *Int. J. Mass Spectrom. Ion Phys.* **1974**, *14*, 459; b) Y. Ikezoe, S. Matsuoka, M. Takebe, A. Viggiano, *Gas-Phase Ion-Molecule Reaction Rate Constants Through 1986*, Maruzen Co. (Japan), **1987**.

[10] V. G. Anicich, *J. Phys. Chem. Ref. Data* **1993**, *22*, 1469.

[11] a) R. G. Cooks, J. H. Beynon, R. M. Caprioli, G. R. Lester, *Metastable Ions*, Elsevier, Amsterdam, **1973**; b) J. L. Holmes, J. K. Terlouw, *Org. Mass Spectrom.* **1980**, *15*, 383; c) J. L. Holmes, *Org. Mass Spectrom.* **1985**, *20*, 169.

[12] a) R. G. Cooks, *Collision Spectroscopy*, Plenum Press, New York, **1978**; b) K. Levsen, H. Schwarz, *Mass Spectrom. Rev.* **1983**, *2*, 77; c) F. W. McLafferty, P. F. Bente, III, R. Kornfeld, S.-C. Tsai, I. Howe, *J. Am. Chem. Soc.* **1973**, *95*, 2120.

[13] S. Dua, S. Peppe, J. H. Bowie, *J. Chem. Soc. Perkin Trans. 2* **2001**, 2244.

[14] a) M. T. Praet, J. C. Lorquet, G. Raşeev, *J. Chem. Phys.* **1982**, *77*, 4611; b) J. Liu, W. Chen, M. Hochlaf, X. Qian, C. Chang, C. Y. Ng, *J. Chem. Phys.* **2003**, *118*, 149.

[15] The narrow peak and its small kinetic energy distribution also account for a non-statistical energy partitioning in the fragment ion, from a synchronous isomerisation→dissociation process. Viewed in this light, ion **1** would undergo back-dissociation into the original CO_2^+ (broad peak) and isomerisation to the exit channel **1a** (narrow peak). If vibrational modes are excited so that **1a** attains the geometry associated with the fragmentation saddle-point, it rapidly decomposes with significant vibrational excitation and a scarce amount of translational energy.

[16] a) W. N. Olmstead, J. I. Brauman, *J. Am. Chem. Soc.* **1977**, *99*, 4219; b) T. F. Magnera, P. Kebarle, *Ionic Processes in the Gas-Phase*, (Ed.: M. A. Almoster Ferreira), D. Reidel, Dordrecht (The Netherlands), **1984**; c) S. T. Graul, M. T. Bowers, *J. Am. Chem. Soc.* **1991**, *113*, 9696; d) J. L. Wilbur, J. I. Brauman, *J. Am. Chem. Soc.* **1991**, *113*, 9699; e) D. M. Cyr, L. A. Posey, G. A. Bishea, C-C Han, M. A Johnson, *J. Am. Chem. Soc.* **1991**, *113*, 9697.

[17] Rearrangement reactions are known to produce more abundant metastable fragmentations than simple bond cleavages that, given the steep rise of k versus E, sample narrow ranges of precursor ion energies for a given rate constants interval. a) W. A. Chupka, *J. Chem. Phys.* **1959**, *30*, 191; b) D. H. Williams, R. G. Cooks, *J. Chem. Soc. Chem. Commun.* **1968**, 663; c) F. W. McLafferty, R. B. Fairweather, *J. Am. Chem. Soc.* **1968**, *90*, 5915.

[18] S. G. Lias, J. E. Bartmess, J. F. Liebman, J. L. Holmes, R. D. Levin, W. G. Mallard, *J. Phys. Chem. Ref. Data* **1988**, *17*, suppl. 1.

[19] S. A. McLuckey, *J. Am. Soc. Mass Spectrom.* **1992**, *3*, 599.

[20] a) D. Krankowsky, K. Mauersberger, *Science* **1996**, *274*, 1324; b) M. H. Thiemens, T. Jackson, K. Mauersberger, B. Schueler, J. Morton, *Geophys. Res. Lett.* **1991**, *18*, 669; c) T. Röckmann, C. A. M. Brenninkmeijer, G. Saueressig, P. Bergamaschi, J. N. Crowley, H. Fisher, P. J. Crutzen, *Science* **1998**, *281*, 544.

[21] J. Farquhar, M. H. Thiemens, T. Jackson, *Science* **1998**, *280*, 1580.

[22] a) T. G. Slanger, L. E. Jusinski, G. Black, G. E. Gadd, *Science* **1988**, *241*, 945; b) X. Yang, J. M. Price, J. A. Mack, C. G. Morgan, C. A. Rogaski, D. McGuire, E. H. Kim, A. M. Wodtke, *J. Phys. Chem.* **1993**, *97*, 3944; c) B. Funke, M. López-Puertas, *J. Geophys. Res. [Atmos.]* **2000**, *105*, 4409; d) C. Nicolas, C. Alcaraz, R. Thissen, J. Zabka, O. Dutuit, *Planet. Space Sci.* **2002**, *50*, 877.

[23] J. E. Bartmess, R. M. Georgiadis, *Vacuum* **1983**, *33*, 149.

[24] a) M. T. Bowers, T. Su, *Interactions between Ions and Molecules*, Plenum Press, New York, **1975**; b) T. Su, J. Chesnavich, *J. Chem. Phys.* **1982**, *76*, 5183.

[25] A. D. Becke, *J. Chem. Phys.* **1993**, *98*, 5648.

[26] P. J. Stephens, F. J. Devlin, C. F. Chablowski, M. J. Frisch, *J. Phys. Chem.* **1994**, *98*, 11623.

[27] B. Mannfors, J. T. Koskinen, L.-O. Pietilä, L. Ahjopalo, *J. Mol. Struct.* **1997**, *393*, 39.

[28] C. W. Bauschlicher, A. Ricca, H. Partridge, S. R. Langhoff in *Recent Advances in Density Functional Theory, Part II* (Ed.: D. P. Chong), World Scientific Publishing Co. (Singapore) **1997**.

[29] R. J. Bartlett, *Annu. Rev. Phys. Chem.* **1981**, *32*, 359.

[30] K. Raghavachari, G. W. Trucks, J. A. Pople, M. Head-Gordon, *Chem. Phys. Lett.* **1989**, *157*, 479.

[31] J. Olsen, P. Jorgensen, H. Koch, A. Balkova, R. J. Bartlett, *J. Chem. Phys.* **1996**, *104*, 8007.

[32] C. Peng, H. B. Schlegel, *Isr. J. Chem.* **1993**, *33*, 449; C. Peng, P. Y. Ayala, H. B. Schlegel, M. J. Frisch, *J. Comput. Chem.* **1996**, *17*, 49.

[33] R. Krishnan, J. S. Binkley, R. Seeger, J. A. Pople, *J. Chem. Phys.* **1980**, *72*, 650; A. D. McLean, G. S. Chandler, *J. Chem. Phys.* **1980**, *72*, 5639; T. Clark, J. Chandrasekhar, G. W. Spitznagel, P. v. R. Schleyer, *J. Comput. Chem.* **1983**, *4*, 294; M. J. Frisch, J. A. Pople, J. S. Binkley, *J. Chem. Phys.* **1984**, *80*, 3265.

[34] M. J. Frisch et al. Gaussian 03, Revision B.04, Gaussian, Inc., Pittsburgh PA, **2003**.

Received: May 17, 2004
Revised: July 30, 2004
Published online: November 5, 2004

